Geometric cues for directing the differentiation of mesenchymal stem cells

Kristopher A. Kilian[a,c], Branimir Bugarija[b,c], Bruce T. Lahn[b,c], and Milan Mrksich[a,c,1]

[a]Department of Chemistry, [b]Department of Human Genetics, and [c]Howard Hughes Medical Institute, The University of Chicago, Chicago, IL 60637

Edited by Laura L. Kiessling, University of Wisconsin-Madison, Madison, WI, and approved January 27, 2010 (received for review March 26, 2009)

Significant efforts have been directed to understanding the factors that influence the lineage commitment of stem cells. This paper demonstrates that cell shape, independent of soluble factors, has a strong influence on the differentiation of human mesenchymal stem cells (MSCs) from bone marrow. When exposed to competing soluble differentiation signals, cells cultured in rectangles with increasing aspect ratio and in shapes with pentagonal symmetry but with different subcellular curvature—and with each occupying the same area—display different adipogenesis and osteogenesis profiles. The results reveal that geometric features that increase actomyosin contractility promote osteogenesis and are consistent with in vivo characteristics of the microenvironment of the differentiated cells. Cytoskeletal-disrupting pharmacological agents modulate shape-based trends in lineage commitment verifying the critical role of focal adhesion and myosin-generated contractility during differentiation. Microarray analysis and pathway inhibition studies suggest that contractile cells promote osteogenesis by enhancing c-Jun N-terminal kinase (JNK) and extracellular related kinase (ERK1/2) activation in conjunction with elevated wingless-type (Wnt) signaling. Taken together, this work points to the role that geometric shape cues can play in orchestrating the mechanochemical signals and paracrine/autocrine factors that can direct MSCs to appropriate fates.

cytoskeleton | microcontact printing | Wnt signaling | microenvironment

Mesenchymal stem cells (MSCs) are multipotent cells that were initially isolated from bone marrow and noted for their ability to differentiate into bone cells (osteoblasts), cartilage cells (chondrocytes), and fat cells (adipocytes) (1, 2). As an autologous source of stem cells, MSCs are under considerable scrutiny for regenerative therapies (3). A combination of physical, chemical, and biological cues present in the stem cell microenvironment have been implicated as directors of stem cell fate in vivo (4). This concept of a stem cell "niche" has motivated empirical studies to identify optimal combinations of extracellular matrix, culture conditions, and temporally administered growth factors to direct stem cell fate in the laboratory (5–7). However, the physical forces and geometry of the MSC microenvironment remain poorly defined and have begun to emerge as critical parameters for regulating cell fate (8, 9).

Physical cues, which were postulated as important factors in tissue development over a century ago (10), have also been recognized as important factors in controlling cell function. Research along these lines has been driven in the past decades with the maturation of microengineering techniques (11–13). Ingber, Whitesides, and colleagues demonstrated the use of substrates that were geometrically patterned to control the microenvironment of individual cells and in turn the decision of cells to initiate apoptosis (14). Patterned substrates have also been used to study cytoskeletal dynamics (15–18) and motility (19–22) with single-cell resolution. Chen and coworkers recently demonstrated the important role that cell shape and size can play in directing the fates of MSCs (23). The degree of cell spreading permitted by the culture density or micro-island size led to a higher degree of cytoskeletal tension and differential expression of the small GTPase RhoA and its downstream effector Rho-associated protein kinase (ROCK) (24). Round cells promoted adipogenesis while cells with high spreading preferred an osteoblast fate. Using other in vitro systems, substrate composition and stiffness (25–27), applied strain (28), cell size and spreading (23, 29–31) have all been shown to influence MSC fate decisions. While adhesion and the degree of cytoskeletal tension are widely accepted as effectors of stem cell fate, the regulatory mechanisms of mechanical-stimulated differentiation is not yet established.

In this work, we demonstrate how shape can be used to promote the differentiation of MSCs to distinct lineages. We treated patterned cells with a mixture of adipogenic and osteogenic differentiation cues and showed differential commitment depends on the adhesive area, aspect ratio, and subcellular curvature. The latter could be used to promote a more contractile cytoskeleton that then promoted an osteogenic outcome whereas shapes of identical area that disrupt contractility favored an adipogenic outcome. A microarray analysis suggested that increased myosin contractility enhances osteogenesis through MAP kinase pathways and Wnt signaling. Together, this work establishes that even subtle shape cues can play a significant role in promoting differentiation.

Results

Differentiation of MSCs on Patterned Monolayers. We used the microcontact printing technique to pattern the shapes of individual cells on a substrate. Briefly, we prepared polydimethylsiloxane (PDMS) stamps that were then used to pattern adhesive islands of octadecanethiolate on a glass cover slip coated with a layer of gold. The remaining regions were then modified with a tri(ethylene glycol)-terminated monolayer followed by immersion of the patterned substrates in a solution of the ECM protein fibronectin to adsorb protein to the hydrophobic islands. MSCs attached to these regions and spread to assume the shape of the underlying island (Fig. S1). Cells remained viable and constrained to the patterns for one week in culture, though at longer times the nonadhesive regions were degraded and cells escaped the pattern and proliferated. To determine if shape alone can induce differentiation within this timeframe, MSCs on the patterned surfaces were exposed to growth media for one week and stained with lineage specific markers (adipocyte/OilRedO (32) and osteoblast/alkaline phosphatase (33)). Under these conditions more than 95% of the MSCs did not show lineage specific staining.

To evaluate differentiation of MSCs using common media supplements unpatterned cells were exposed to adipogenesis and osteogenesis-promoting soluble cues and a 1:1 combination of

Author contributions: K.A.K., B.T.L., and M.M. designed research; K.A.K. and B.B. performed research; B.B. contributed new reagents/analytic tools; K.A.K., B.B., and M.M. analyzed data; and K.A.K. and M.M. wrote the paper.

The authors declare no conflict of interest.

This article is a PNAS Direct Submission.

Freely available online through the PNAS open access option.

[1]To whom correspondence should be addressed. E-mail: mmrksich@uchicago.edu.

This article contains supporting information online at www.pnas.org/cgi/content/full/0903269107/DCSupplemental.

www.pnas.org/cgi/doi/10.1073/pnas.0903269107

both (the "mixed media"). The culture was stopped after one week and the cells were stained to reveal that MSCs differentiated to the defined lineage and cells exposed to the mixed media show a mixture of both lineages (Fig. S2). The remaining experiments were performed using patterned cells exposed to mixed media containing these competing soluble differentiation cues.

Directing MSC Differentiation with Geometric Cues. We first identified the appropriate size of a patterned feature that would show little bias in directing cell differentiation towards osteogenic and adipogenic fates. Cells that were adherent to mixed shapes with a range of geometric features and having areas of 1,000, 2,500 and, 5,000 μm^2 were treated with mixed media for one week and then probed with lineage specific markers. In all cases, approximately 50–60% of the cells had differentiated, but with different fates. For the small islands we observed primarily adipocyte characteristics (lipid vacuoles) while the large islands promoted an osteoblast fate (alkaline phosphatase), consistent with the report by Chen and coworkers that cell size has a strong influence on differentiation (23) (Figs. S3 and S4). For cells on patterns of intermediate area (2,500 μm^2) the differentiation proceeded to give a mixed population of adipocytes and osteoblasts. We next compared differentiation of MSCs on a series of shapes that maintained this constant area but that displayed differences in aspect ratio and curvature.

Patterned cells that were cultured for one week in mixed media on rectangles having aspect ratios of 1:1, 3:2 and 4:1 showed that the yield of osteogenesis increased with aspect ratio. Cells in squares (aspect ratio 1:1) showed 46% osteogenesis while cells on rectangles having aspect ratios of 3:2 and 4:1 displayed 56% and 61% osteogenesis, respectively (Fig. 1*A*). We next evaluated the influence of three shapes that each had pentagonal symmetry but with different types of curvature (Fig. 1*B*). The first shape approximated a flower with large convex curves along each edge. For this shape, 62% of MSCs differentiated to give adipocytes with the balance yielding osteoblasts. Cells patterned into a pentagon shape—with straight lines for the edges—showed an even distribution of adipocytes and osteoblasts. Cells having a shape approximating a star—with concave edges and sharp points at the vertices—had a 62% preference for an osteogenic fate. In all cases, a small portion of differentiated cells (~10%) displayed both markers and were not used in the analysis. This experiment is striking because the three shapes had a constant area and only subtle geometric differences yet had a significant difference in directing lineage commitment. Significantly, the medium and soluble factors were unchanged in these experiments, showing that the shape cues imposed by the underlying pattern were alone responsible for changing the fate of the cells. This trend is consistent with our earlier study that showed an increasingly contractile cytoskeleton in cells as they moved from a flower to a pentagon and finally to a star shape (18). In these experiments we used visual inspection to mark cells as adipocytes or osteoblasts, (or neither), as has been common in other studies (23). To verify that this process reliably categorized the cells, we also repeated the analysis using an automated image analysis algorithm. We acquired color images of individual cells and performed a color deconvolution to separate the red and purple channels for images of each dually stained cell (see *SI Text* and Fig. S5 for details). Fig. 1*C* shows histograms of color-specific intensities for the flower and star shapes. We assigned fixed thresholds for designating lineage and report populations of cells that show either of the stains, a combination of both, or neither. The trend in differentiation determined in this manner is comparable to that obtained by visual inspection and therefore provides strong evidence that shape alone is influencing the differentiation of adherent cells. For experiments that follow, we find that the fraction of cells that display either both or neither stains is approximately constant and we therefore show only the relative populations of cells displaying one or the other marker.

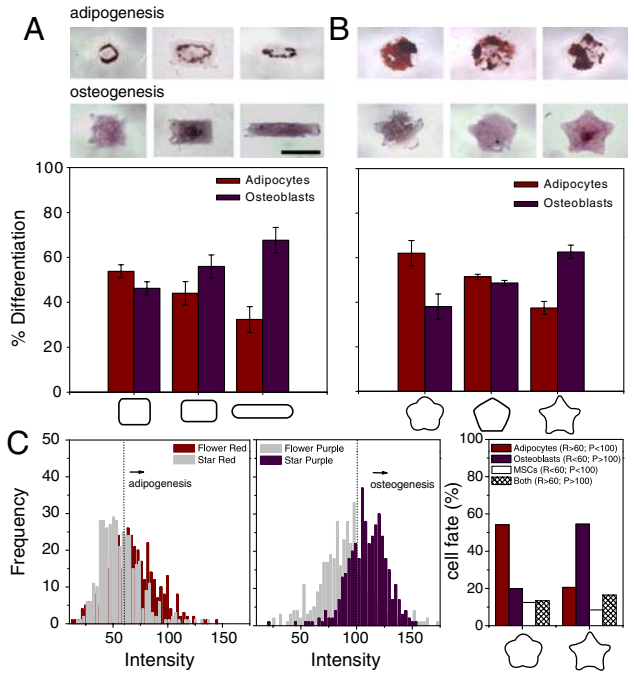

Fig. 1. (*A*) Percentage of cells captured on rectangles of varying aspect ratio differentiating to adipocyte or osteoblast lineage. (*B*) Percentage of cells differentiating to either lineage when captured on fivefold symmetric shapes. (*C*) Comparison of color intensity histograms generated by measuring the red and purple channels of cells in flower and star shapes ($n = 393$). The *dotted line* represents thresholds used to define lineage specification. The *bar graph* summarizes lineage assignment from these cells using this method (R = red channel, P = purple channel). Error bars are standard deviations from four separate experiments with over 200 cells per shape, *p*-value <0.005. (Scale bar, 50 μm).

Influence of Shape on Cytoskeleton in MSCs. We next characterized the cytoskeletal organization in MSCs on different shapes. Cells were cultured for 6 h under standard growth conditions and then fixed and probed by immunofluorescence to observe the stress fibers and the focal adhesion complexes. Fig. 2*A–C* shows immunofluorescent images of cells cultured on 2,500 μm^2 islands stained for actin (green), vinculin (red), and merged images with nuclei in blue. Previous work using patterned substrates has shown that cells assemble stress fibers along edges that overlap regions of substrate that are nonadhesive (15, 18). In the flower shape, stress fibers predominate at the acute corners between petals where the cell spans nonadhesive regions. In sharp contrast to the flower shape, the concave regions between points of the star give rise to highly contractile regions where the cell spans across the nonadhesive area. Similar results were obtained with increasing aspect ratio and contractility (Fig. S6). To assess differences in patterns of focal adhesion and stress fibers between cells, immunofluorescent heatmaps were generated for >80 cells per shape (Fig. S7). On average, cells in star shapes show larger focal adhesions and stress fibers than cells in flower shapes. We note that our finding is in contrast to a study by Chen and coworkers (17) that found that cell size, but not shape, governs the amount of focal adhesion. These results may stem from the use of different cell lines, and perhaps a greater sensitivity of the MSCs to shape.

Immunofluorescent staining of myosin IIa, the primary motor protein assembly that is responsible for cell contractility, was performed for MSCs adherent to the shapes (Fig. 2*D*). Average myosin IIa fluorescent heatmaps from a large number of cells demonstrate a higher degree of actomyosin contractility along the edges that overlap the nonadhesive regions of the monolayer for cells on star shapes (Fig. 2*E*). These results suggest regions of

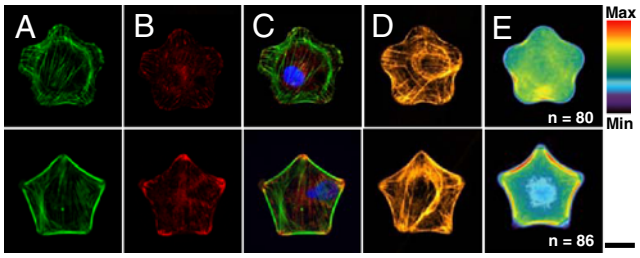

Fig. 2. (*A*)-(*C*) Immunofluorescent images of cells in flower and star shapes stained for F-actin (*green*), vinculin (*red*) and nuclei (*blue*). (*D*) Immunofluorescent images of cells in flower and star shapes stained for myosin IIa. (*E*) Fluorescent heatmaps of >80 cells stained for myosin IIa as a quantitative measure of contractility. (Scale bar, 20 μm).

local curvature on shapes that increase cytoskeletal tension of adherent cells promote osteogenesis relative to adipogenesis. The heatmaps show a slight variation (16% for the star and 23% for the flower) in the intensities for symmetrical features. The heatmaps were constructed from cells that retained their relative alignment in the culture and therefore the asymmetry may reflect either a global polarization or intrinsic variability in cytoskeletal structure of patterned cells within a sample. We have not performed experiments to address this question.

Modulating Differentiation by Cytoskeletal Manipulation. We have shown that the cytoskeleton in adherent cells is strongly influenced by subtle geometric shape cues, and suggest that the osteogenic program in the cells is directly dependent on a contractile cytoskeleton. To further address this possibility, we evaluated the effect of several pharmacological agents that are known to modulate the cytoskeleton. Inhibitors were added to cell culture media at concentrations that allowed complete spreading of the MSC to the underlying shape with no visually apparent changes to morphology. Control cultures without pharmacological agents show 72% of cells on the flower shape have an adipogenic fate compared to 67% of cells on the star shape showing an osteogenic fate (Fig. 3*A*). We then compared the shape-dependent differentiation of cells that were treated with nocodazole, a potent microtubule depolymerizing agent that has been shown to increase cell contractility (34). Indeed, the drug removed the influence of shape and in all cases gave a strong preference for osteogenesis (>80%) (Fig. 3*B*). Cytochalasin D is a small molecule that inhibits F-actin polymerization and therefore reduces contractility of the actin cytoskeleton. This agent again removed the effect of shape on differentiation but this time favored an adipogenic fate for cells on all shapes (Fig. 3*C*). Two other drugs that directly inhibit contractility—blebbistatin, which inhibits myosin II and Y-27632, which inhibits ROCK—caused a decrease in osteogenesis with a corresponding increase in cells with adipocyte phenotypes and again removed the influence of shape on differentiation (>70%, Fig. 3*D*, *E*). Finally, we treated MSCs with an antibody against the α5β1 integrin—which mediates coupling of the cytoskeleton to the extracellular matrix—prior to adhesion, but using a concentration of antibody that does not block spreading of the cell to fill the patterned island (35). We find that for both shapes, approximately 85% of the cells choose an adipogenic fate (Fig. 3*F*). Treatment of cells on shapes with varying aspect ratio with these agents shows the same trend (Fig. S8). Each of these results is consistent with the role of actomyosin contractility in promoting an osteogenic fate in cells, and further serves to establish the apparent requirement for actomyosin contractility in shape-dependent influence on differentiation.

RNA Expression Analysis of Cells on Flower and Star Shapes. Our observations showing that osteogenesis is promoted by an increased cytoskeletal contractility is consistent with previous reports de-

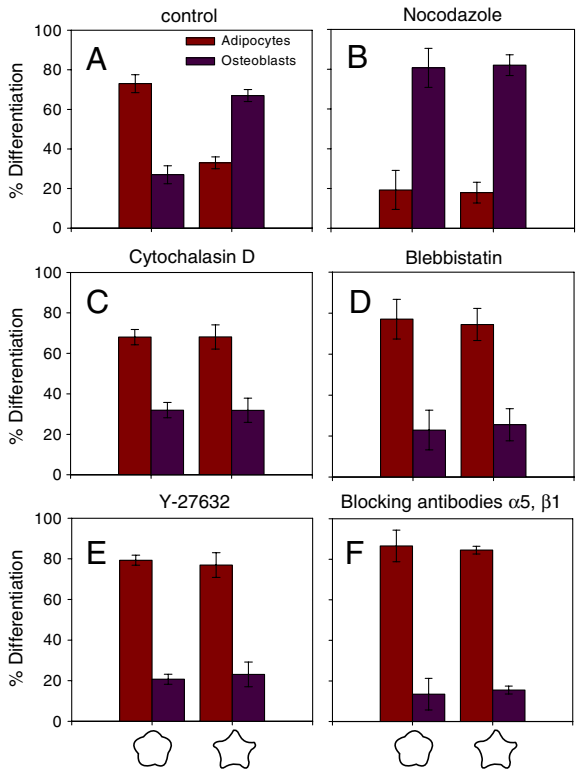

Fig. 3. (*A*) Percentage of cells differentiating to adipocytes or osteoblasts when cultured on patterns of the same shape, *p*-value <0.01. (*B*)-(*E*) Effect on shape-promoted differentiation in the presence of cytoskeleton disruptors and (*F*) integrin blocking antibodies.

monstrating that stiff substrates promote osteogenesis (and which is intuitively linked to the physical characteristics of bone) (23, 27). To gain an insight on how actomyosin contractility regulates the osteogenesis program, we performed a gene expression analysis to establish the differentiated states of the MSCs and, as described further below, to identify gene families that were important in mediating the effect of shape on differentiation. RNA was isolated from cells grown on 12 identical patterned substrates (maximum 2,500 cells/substrate) that were exposed for 1 week to mixed media on flower shapes, star shapes, and nonpatterned controls. When isolating RNA, we selected cultures wherein greater than 90% of the cells were attached to individual features and had spread to take on the shape of the feature. In this way, RNA derived from incompletely spread cells represented a minor fraction of the pool and was not expected to significantly alter the expression profiles of the patterned cells. After one round of amplification, we analyzed the RNA transcripts by hybridization to Affymetrix GeneChips and analyzed the relative expression levels of known markers. A panel of common adipogenic transcripts showed higher levels of expression in cells cultured on the flower shape relative to the star and unpatterned surfaces (normalized to growth media control, Fig. 4*A*. See Table S1 for fold change values). Similarly, a group of osteogenic transcripts displayed higher expression for cells cultured in star shapes. The trend in expression level across lineage specific transcripts is consistent with the histological staining. To supplement the differential expression of lineage specific transcripts we additionally performed immunofluorescent staining and RT-PCR (Fig. S9). Immunofluorescent staining of peroxisome proliferator-activated receptor γ (PPAR γ) and Runt-related transcription factor 2 (Runx2)—markers for adipogenesis and osteogenesis that were differentially expressed in the microarray data—reveal a comparable trend to the histology stains in shape directed differentiation. The RT-PCR gels show increased expression of osteocalcin

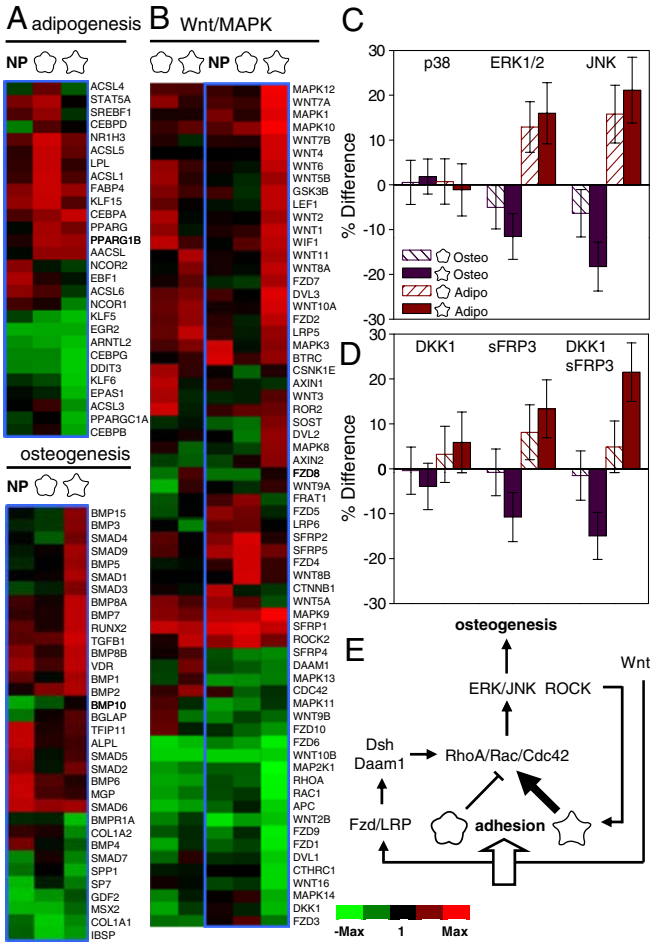

Fig. 4. Hierarchical clustering of (*A*) osteogenic and adipogenic transcripts expressed in cells captured to both shapes and (*B*) MAP kinase and Wnt signaling transcripts: *Left*—cells in flower and star shapes cultured in standard growth media for 1 week. *Right* (*blue outline*)—after 1 week exposure to mixed adipogenic and osteogenic media. (*C*) Change in differentiation from control when exposed to MAPK inhibitors. (*D*) Change in differentiation of cells in the presence of Wnt antagonists. (*E*) Speculative pathway for shape directed differentiation of adherent MSCs.

(BGLAP) for cells in star shapes and lipoprotein lipase (LPL) for cells in flower shapes, consistent with the microarray results (Fig. S9*D*).

A comparison of the gene expression profiles in cells that were adherent to star and flower shapes, but that were not yet treated with the differentiation cues shows significant differential expression of genes associated with Wnt signaling and mitogen-activated protein kinase cascades (MAPK), both of these pathways are well-studied in mechanotransduction and osteogenic regulation (36). In the absence of soluble lineage guidance cues, both shapes express transcripts associated with MAPK and Wnt signaling, but cells adherent to the star shape express higher levels of *noncanonical* (also known as Planar Cell Polarity (PCP) pathway) Wnt associated transcripts including: Rac1, cell division cycle 42 (Cdc42), RhoA, ROCK2, dishevelled 1, 2, and 3 (DVL1, 2, and 3) and dishevelled associated activator of morphogenesis 1 (DAAM1). The higher expression of the GTPases involved in cell motility, Rac, and Cdc42, is consistent with recent work in our group that established greater polarity and protrusion with cells in a star geometry (18). Wnt11, the major player in the *noncanonical* PCP pathway, also shows >10-fold expression compared to cells adherent to the flower shape. Further, those cells adherent to the star shape have higher expression of Wnt receptors including LRP5 and 8 out of 10 Frizzled receptors (FZD). (Fig. 4*B*, left and Table S2). Previous work has demonstrated the importance of Wnt signaling in regulating actomyosin contractility (37). Furthermore, high levels of the *noncanonical* Wnt downstream effector ROCK has been shown to trigger osteogenesis through a myosin-generated tension feedback loop (23, 38). It is therefore reasonable to suggest that contractile cells may be poised in a state of higher susceptibility to soluble factors including autocrine/paracrine Wnt signals as well as osteogenic media supplements.

Cells that were exposed to mixed media show significantly different expression profiles compared to patterned cells that had not been treated with soluble differentiation cues (Fig. 4*B*, blue box). Of particular interest, MSCs cultured on stars show elevated expression of genes involved in the MAP kinase pathways linked to both mechanotransduction and osteogenesis (39) including: extracellular signal-regulated kinases ERK1/2 (MAPK1, MAPK3), c-Jun N-terminal kinases JNK (MAPK8, MAPK9, MAPK10) and p38 kinases (MAPK11, MAPK12, MAPK13, MAPK14). We also find that star-shaped cells display higher expression of 12 of the 17 Wnt transcripts and downstream effectors of both the *canonical* and *noncanonical* pathways. In contrast, flower-shaped cells display increased expression of dikkopf-1 (DKK1) and all of the secreted frizzled-related proteins (sFRP) involved in Wnt antagonism (see Table S2 for fold change values).

Inhibition of MAPK and Wnt Signaling in Patterned Cells. To determine the extent to which MAP kinase cascades and Wnt signaling play a role in shape-promoted osteogenesis, we tested the effect of inhibitors of these pathways on the differentiation. Addition of SB202190 a specific inhibitor of p38 phosphorylation (40) resulted in no discernible change in lineage commitment (Fig. 4*C*) whereas the ERK 1/2 inhibitor FR180204 and the JNK 1/2/3 inhibitor SP600125 (41) caused a decrease in osteogenesis with a concurrent increase in adipogenesis demonstrating the importance of these cascades in osteoblast differentiation.

We also probed the role of Wnt signaling by supplementing the media with the recombinant extracellular Wnt antagonists DKK1 and sFRP3 (42). Treatment with DKK1 caused a slight decrease in osteogenesis and increase in adipogenesis relative to control (Fig. 4*D*). Incubation in the presence of sFRP3 caused a greater decrease in osteogenesis with an associated increase in adipogenesis. Combining both DKK1 and sFRP3 led to a further increase in adipogenesis relative to control. Importantly, treatment with Wnt inhibitors abrogated star-shape-promoted trends in osteogenesis. From these results we speculate that cell contractility elevates ERK/JNK cascades and makes MSCs in star shapes more susceptible to secreted molecules (Fig. 4*E*).

Limits of Geometric Control over MSC Fate. The studies described above used shapes that yielded differentiation of approximately 60–70% of one fate. We asked whether shapes that combined local curvature with aspect ratio could increase the preference for the major outcome. Therefore, we compared the differentiation of cells on a circular shape and a "holly leaf" that incorporates two osteogenesis-promoting cues: moderate aspect ratio (2:1) and regions of subcellular curvature and concavity. Immunofluorescence staining shows that cells confined to the holly shape have larger focal adhesions and stress fibers spanning the nonadhesive regions compared to cells in circular patterns (Fig. S10). Further, heat maps showing the localization of myosin IIa show a striking difference in the contractility state of the cells (Fig. 5*A*). MSCs on both shapes were exposed to mixed media for 1 week and stained for markers of osteogenesis and adipogenesis. Cells in the circular island favored the adipogenic fate (74%) while the contractile cells in the holly shape favored the osteogenic fate (67%) (Fig. 5*B*). The difference in differentiation between these shapes is approximately equal to that observed with the flower and star shape. Thus, we infer that under the conditions employed in our work, we are realizing the maximum influence that shape

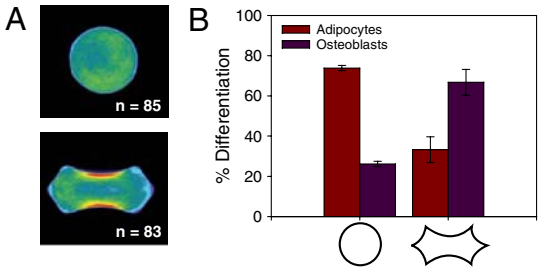

Fig. 5. (*A*) Myosin IIa immunofluorescent heat maps of >80 cells cultured in circles or holly shapes. (*B*) Corresponding differentiation of cells in both shapes after exposure to mixed media, *p*-value <0.005.

can have in directing differentiation. We would expect, however, that synergistic combinations of growth factors and small molecules in conjunction with geometric cues can achieve a more specific outcome.

Discussion

In this paper we used patterned cells to investigate the relationship between shape and differentiation of multipotent MSCs. The patterned monolayers provide exquisite control over the shapes of individual cells, thereby enabling statistically relevant observations over a large number of cells in a single well of a tissue culture plate. In this study, we varied the aspect ratio and subcellular curvature of individual cells and could include multiple shapes on a single substrate. MSCs survived and remained confined to patterns for a week allowing introduction of differentiation inducing chemical cues. We found that shapes promoting increased contractility led to preferential osteogenesis when cells were exposed to a mixture of lineage cues. In contrast, cells in shapes that promote low contractility preferred to follow an adipocyte lineage.

The influence of geometry on differentiation that we observe is consistent with a model wherein the local shape cues (i.e. pointed features between concave regions) promote increased myosin contractility which enhances pathways associated with osteogenesis. Immunofluorescence analysis of the cells, for example, confirms the relationship between the shape cues and the enhanced stress filaments in the patterned cells (Fig. 2 and Fig. S7). Treatment of the cells with cytoskeletal-disrupting agents gave results that are also consistent with this model. Nocodazole, for example, increases the contractility of the cytoskeleton and was shown to drive the majority of MSCs in shapes towards osteoblast fate. In contrast, cells exposed to molecules that inhibit contractility tended to differentiate into adipocytes. Further, by blocking a portion of cell surface integrin receptor with an antibody, we could decrease the tension exerted by the cell on the substrate with a corresponding inhibition of osteogenesis. Taken together these results demonstrate the importance of adhesion and a highly contractile state for bone cell formation.

This interpretation is also consistent with the report by Chen and coworkers showing that myosin-generated cytoskeletal tension that follows spreading of MSCs leads to higher levels of RhoA, ROCK, and myosin light chain phosphorylation (23). This tension-specific feedback loop was shown to act as a switch for osteogenesis. Further, a very recent report by Chien and coworkers studied the differentiation of MSCs on titanium oxide nanotubes and found that larger tubes led to an increased spreading of cells and a corresponding increase in osteogenesis (31). Discher and coworkers varied the stiffness of the underlying matrix in MSC culture and showed elasticity to be a powerful mechanical cue in directing MSC fate (27). Stiff matrices lead to enhanced cytoskeletal tension and osteogenesis while softer matrices directed MSCs towards alternative lineages. Interestingly, the synthetic and natural matrices that had a comparable directing effect in cell fate also shared a similar stiffness. We note the temptation to speculate that cells differentiate in response to shape cues in a fashion that is consistent with the native geometry of cells of that lineage—for example, round shapes with low stress promote fat cells and contractile pointed shapes promote bone—but we have no direct evidence to support this notion. In any event, this body of work demonstrates the significant roles that physical cues can play to increase cytoskeletal tension in the MSC microenvironment and the relevance of these effects to promoting osteogenesis.

To aid in understanding the role that shape plays in regulating MSC differentiation, we performed gene expression analysis using DNA microarrays. After exposing patterned cells to mixed media containing adipogenic/osteogenic soluble cues we see a higher degree of osteogenic transcript expression for cells cultured in star shapes and higher expression levels of adipogenic transcripts in cells on flower shapes, consistent with the histological studies. In both cases of normal media and mixed media, microarray analysis reveals differential gene expression for transcripts associated with MAP kinase pathways and Wnt signaling suggesting a role for secreted factors. In particular, we find that cells cultured on star shapes in growth media promote expression of *noncanonical* Wnt/Fzd signaling molecules (including downstream effectors RhoA and ROCK previously shown to be involved in osteogenesis (23, 38)). Moreover, when exposed to mixed media the gene expression of tension specific MAP kinases (p38, ERK1/2, JNK) and both *canonical* and *noncanonical* Wnt transcripts is increased for cells on star shapes relative to those on flower shapes and on unpatterned surfaces. In contrast, cells in flower shapes show elevated expression of Wnt inhibitory molecules (sFRPs), suggesting that this geometry may stimulate functional Wnt antagonism.

Wnt signaling is known to be important in osteoblast differentiation (36). Recent studies have also shown how Wnts are activated by mechanical stimuli during bone development (43, 44) with additional functions in regulating cell contractility during tissue morphogenesis (37, 45). p38, ERK, and JNK cascades are known to be activated by mechanical stimuli but have also been implicated as targets of Wnt signaling through *canonical* (40) and *noncanonical* pathways (41, 46, 47) for regulation of osteogenesis. Taken together, these studies and our results support a picture where actomyosin contractility stimulates MAPK cascades and Wnt signaling to regulate osteoblast differentiation.

To support this hypothesis, treatment of cells in both shapes with MAP kinase inhibitors shows that ERK1/2 and JNK are important for osteogenesis and their inhibition causes increased adipogenesis when exposed to mixed media. This result is consistent with previous studies that point to the important role of ERK1/2 and JNK in osteogenesis (41, 46, 48, 49) as well as an inhibitory role of JNK in adipogenesis (49). As further support, Wnt inhibition by DKK1 and sFRP3 led to a decrease in osteogenesis with a concurrent increase in adipogenesis. From these results, we propose that cells in star shapes increase the levels of the *noncanonical* Wnt signaling molecules, their receptors, and their downstream effectors. Subsequently, activation of ERK/JNK by soluble cues and autocrine/paracrine Wnt signaling is enhanced for cells in this geometry leading to elevated expression of master osteoblast regulators (see Fig. 4*E*). Likewise, it appears that cells in geometries associated with low contractility may not only make the cells more susceptible to soluble adipogenic cues but may also promote negative regulation of Wnt signaling via the secretion of sFRPs.

This work has harnessed the utility of microcontact printing to control cell shape and allow systematic and highly parallel studies of the factors that affect stem cell fate. This technique is also notable because it can be used to study large populations of cells, providing good statistical data, and even providing sufficient RNA to permit gene expression profiling. By keeping the area and shape of cells constant, the heterogeneities that normally attend cell cultures are reduced, giving a targeted investigation of the synergy between cell shape, biological, and chemical signals.

Differentiation media supplements have been shown to operate through temporal regulation of different signaling cascades (48). Histology staining and RNA expression analysis shows high levels of activation in one week compared to unpatterned cells under the same media conditions. Thus the use of shape cues can be employed to enhance and rationally control differentiation specific signaling, thereby accelerating biochemical assays and guided differentiation in engineered scaffolds. Therefore, this study provides both unique tools and methodologies for investigative biology as well as design principles that will prove useful for designing materials for regenerative medicine.

Materials and Methods

Further details of materials and methods are included in *SI Text*.

Cell Culture. Human MSCs were a gift from Dr. Andy Xiang Peng at Sun Yat-Sen University, and derived as described (33). Cells were cultured in DMEM-low glucose supplemented with 10% FBS, 1% penicillin/streptomycin, passaged at 70–80% confluency and seeded at ~5, 000 cells/cm^2. Differentiation media was added by itself or as a 1:1 (v/v) combination.

Surface Preparation. Microcontact printing of self-assembled monolayers on thin gold layers was performed as described previously (18).

Histology. Cells were fixed with 4% formaldehyde and stained for adipogenesis (lipid droplets, Oil Red O), and osteogenesis (alkaline phosphatase, BCIP/NBT) per manufacturer's instructions.

ACKNOWLEDGMENTS. We thank Dr. Vytas Bindokas for assistance with microscopy data analysis. This work was funded by the National Cancer Institute of the National Institutes of Health. K.A.K. is supported by a Ruth L. Kirstein National Research Service Award Number F32GM087048 from the National Institute of General Medical Sciences. Photolithography was performed at the Chicago Materials Research Science and Engineering Centers microfluidic facility (National Science Foundation).

1. Meirelles LdS, Chagastelles PC, Nardi NB (2006) Mesenchymal stem cells reside in virtually all post-natal organs and tissues. *J Cell Sci* 119:2204–2213.
2. Crisan M, et al. (2008) A perivascular origin for mesenchymal stem cells in multiple human organs. *Cell Stem Cell* 3:301–313.
3. Kassem M (2006) Stem cells: Potential therapy for age-related diseases. *Ann N Y Acad Sci* 1067:436–442.
4. Ohlstein B, Kai T, Decotto E, Spradling A (2004) The stem cell niche: Theme and variations. *Curr Opin Cell Biol* 16:693–699.
5. Pittenger MF, et al. (1999) Multilineage potential of adult human mesenchymal stem cells. *Science* 284:143–147.
6. Caplan AI, Bruder SP (2001) Mesenchymal stem cells: Building blocks for molecular medicine in the 21st century. *Trends Mol Med* 7:259–264.
7. Derda R, et al. (2007) Defined substrates for human embryonic stem cell growth identified from surface arrays. *ACS Chem Biol* 2:347–355.
8. Graziano A, et al. (2007) Concave pit-containing scaffold surfaces improve stem cell-derived osteoblast performance and lead to significant bone tissue formation. *PLoS One* 2(6):e496 1–9.
9. McBride SH, Falls T, Knothe Tate ML (2008) Modulation of stem cell shape and fate b: Mechanical modulation of cell shape and gene expression. *Tissue Eng Pt A* 14:1573–1580.
10. Wolff J (1986) *The law of bone remodelling*, ed Maquet P (Springer-Verlag and Heidelberg GmbH and Co., Berlin), pp 1–126.
11. O'Neill C, Jordan P, Ireland G (1986) Evidence for two distinct mechanisms of anchorage stimulation in freshly explanted and 3T3 swiss mouse fibroblasts. *Cell* 44:489–496.
12. Ingber DE (2006) Mechanical control of tissue morphogenesis during embryological development. *Int J Dev Biol* 50:255–266.
13. Spatz JP, Geiger B (2007) Molecular engineering of cellular environments: Cell adhesion to nano-digital surfaces. *Methods Cell Biol* 83:89–111.
14. Chen CS, Mrksich M, Huang S, Whitesides GM, Ingber DE (1997) Geometric control of cell life and death. *Science* 276:1425–1428.
15. Thery M, Pepin A, Dressaire E, Chen Y, Bornens M (2006) Cell distribution of stress fibres in response to the geometry of the adhesive environment. *Cell Motil Cytoskeleton* 63:341–355.
16. Parker KK, Tan J, Chen CS, Tung L (2008) Myofibrillar architecture in engineered cardiac myocytes. *Circ Res* 103:340–342.
17. Chen CS, Alonso JL, Ostuni E, Whitesides GM, Ingber DE (2003) Cell shape provides global control of focal adhesion assembly. *Biochem Biophys Res Commun* 307:355–361.
18. James J, Goluch ED, Hu H, Liu C, Mrksich M (2008) Subcellular curvature at the perimeter of micropatterned cells influences lamellipodial distribution and cell polarity. *Cell Motil Cytoskeleton* 65:841–852.
19. Brock A, et al. (2003) Geometric determinants of directional cell motility revealed using microcontact printing. *Langmuir* 19:1611–1617.
20. Parker KK, et al. (2002) Directional control of lamellipodia extension by constraining cell shape and orienting cell tractional forces. *FASEB J* 16:1195–1204.
21. Jiang X, Bruzewicz DA, Wong AP, Piel M, Whitesides GM (2005) Directing cell migration with asymmetric micropatterns. *Proc Natl Acad Sci USA* 102:975–978.
22. Kandere-Grzybowska K, et al. (2007) Cell motility on micropatterned treadmills and tracks. *Soft Matter* 3:672–679.
23. McBeath R, Pirone DM, Nelson CM, Bhadriraju K, Chen CS (2004) Cell shape, cytoskeletal tension, and RhoA regulate stem cell lineage commitment. *Dev Cell* 6:483–495.
24. Bhadriraju K, et al. (2007) Activation of ROCK by RhoA is regulated by cell adhesion, shape, and cytoskeletal tension. *Exp Cell Res* 313:3616–3623.
25. Murphy WL, Hsiong S, Richardson TP, Simmons CA, Mooney DJ (2004) Effects of a bone-like mineral film on phenotype of adult human mesenchymal stem cells in vitro. *Biomaterials* 26:303–310.
26. Connelly JT, Garcia AJ, Levenston ME (2008) Interactions between integrin ligand density and cytoskeletal integrity regulate BMSC chondrogenesis. *J Cell Physiol* 217(1):145–154.
27. Engler AJ, Sen S, Sweeney HL, Discher DE (2006) Matrix elasticity directs stem cell lineage specification. *Cell* 126:677–689.
28. Ward DF, Jr, et al. (2007) Mechanical strain enhances extracellular matrix-induced gene focusing and promotes osteogenic differentiation of human mesenchymal stem cells through an extracellular-related kinase-dependent pathway. *Stem Cells Dev* 16:467–480.
29. Yang Y, Relan NK, Przywara DA, Schuger L (1999) Embryonic mesenchymal cells share the potential for smooth muscle differentiation: Myogenesis is controlled by the cell's shape. *Development* 126:3027–3033.
30. Ni XF, et al. (2008) On-chip differentiation of human mesenchymal stem cells into adipocytes. *Microelectron Eng* 85:1330–1333.
31. Oh S, et al. (2009) Stem cell fate dictated solely by altered nanotube dimension. *Proc Natl Acad Sci USA*, 106(7) pp:2130–2135.
32. Yu W, et al. (2008) Critical role of phosphoinositide 3-kinase cascade in adipogenesis of human mesenchymal stem cells. *Mol Cell Biochem* 310:11–18.
33. Zhang A-X, et al. (2007) Proteomic identification of differently expressed proteins responsible for osteoblast differentiation from human mesenchymal stem cells. *Mol Cell Biochem* 304:167–179.
34. Chang Y-C, Nalbant P, Birkenfeld J, Chang Z-F, Bokoch GM (2008) GEF-H1 couples nocodazole-induced microtubule disassembly to cell contractility via RhoA. *Mol Biol Cell* 19:2147–2153.
35. Feng Y, Mrksich M (2004) The synergy peptide PHSRN and the adhesion peptide RGD mediate cell adhesion through a common mechanism. *Biochemistry* 43:15811–15821.
36. Hartmann C (2006) A Wnt canon orchestrating osteoblastogenesis. *Trends Cell Biol* 16:151–158.
37. Lee J-Y, et al. (2006) Wnt/frizzled signaling controls c. Elegans gastrulation by activating actomyosin contractility. *Curr Biol* 16:1986–1997.
38. Arnsdorf EJ, Tummala P, Kwon Ronald Y, Jacobs CR (2009) Mechanically induced osteogenic differentiation—the role of RhoA, ROCKII and cytoskeleton dynamics. *J Cell Sci* 122:546–553.
39. Jaiswal RK, et al. (2000) Adult human mesenchymal stem cell differentiation to the osteogenic or adipogenic lineage is regulated by mitogen-activated protein kinase. *J Biol Chem* 275:9645–9652.
40. Caverzasio J, Manen D (2007) Essential role of Wnt3a-mediated activation of mitogen-activated protein kinase p38 for the stimulation of alkaline phosphatase activity and matrix mineralization in C3H10T1/2 mesenchymal cells. *Endocrinology* 148:5323–5330.
41. Fu L, et al. (2008) Stimulation of osteogenic differentiation and inhibition of adipogenic differentiation in bone marrow stromal cells by alendronate via ERK and JNK activation. *Bone* 43:40–47.
42. Alfaro MP, et al. (2008) The Wnt modulator sFRP2 enhances mesenchymal stem cell engraftment, granulation tissue formation and myocardial repair. *Proc Natl Acad Sci USA* 105:18366–18371.
43. Hens JR, et al. (2005) TOPGAL mice show that the canonical Wnt signaling pathway is active during bone development and growth and is activated by mechanical loading in vitro. *J Bone Miner Res* 20:1103–1113.
44. Robinson JA, et al. (2006) Wnt/beta -catenin signaling is a normal physiological response to mechanical loading in bone. *J Biol Chem* 281:31720–31728.
45. Wozniak MA, Chen CS (2009) Mechanotransduction in development: A growing role for contractility. *Nat Rev Mol Cell Biol* 10:34–43.
46. Chang J, et al. (2007) Noncanonical Wnt-4 signaling enhances bone regeneration of mesenchymal stem cells in craniofacial defects through activation of p38 MAPK. *J Biol Chem* 282:30938–30948.
47. Bikkavilli RK, Feigin ME, Malbon CC (2008) $G\alpha_o$ mediates WNT-JNK signaling through Dishevelled 1 and 3, RhoA family members, and MEKK 1 and 4 in mammalian cells. *J Cell Sci* 121:234–245.
48. Jaiswal RK, et al. (2000) Adult human mesenchymal stem cell differentiation to the osteogenic or adipogenic lineage is regulated by mitogen-activated protein kinase. *J Biol Chem* 275:9645–9652.
49. Tominaga S, Yamaguchi T, Takahashi S-I, Hirose F, Osumi T (2005) Negative regulation of adipogenesis from human mesenchymal stem cells by Jun N-terminal kinase. *Biochem Biophys Res Commun* 326:499–504.